Synthesis of high functionality and quality mannose-grafted lipids to produce macrophage-targeted liposomes

Masayori Hagimori[a,*], Yorinao Chinda[a], Tadaharu Suga[a], Kazuto Yamanami[a], Naoya Kato[a], Tatsuo Inamine[b], Yuki Fuchigami[a], Shigeru Kawakami[a,*]

[a]*Department of Pharmaceutical Informatics, Graduate School of Biomedical Sciences, Nagasaki University, 1-7-1 Sakamoto, Nagasaki 852-8501, Japan*
[b]*Department of Pharmacotherapeutics, Graduate School of Biomedical Sciences, Nagasaki University, 1-7-1 Sakamoto, Nagasaki 852-8501, Japan*

***Corresponding authors:**
Masayori Hagimori (e-mail: hagimori@nagasaki-u.ac.jp)
Shigeru Kawakami (e-mail: skawakam@nagasaki-u.ac.jp)

Keywords: mannose; lipid; serine–glycine repeat spacer; macrophage; liposome

ABSTRACT

The mannose receptor, which is responsible for tumor invasion, proliferation, and metastasis in the tumor microenvironment, is overexpressed in tumor-associated macrophages. Mannose is commonly applied to PEGylated liposomes in macrophage-targeted cancer therapy. To develop a high functionality and quality (HFQ) lipid for macrophage-targeted liposomes, we designed a novel mannosylated lipid with improved mannose receptor binding affinity using serine–glycine repeats $(SG)_n$. We synthesized Man(S)-$(SG)_5$-SSK-K$(Pal)_2$ using only a fluorenylmethyloxycarbonyl (Fmoc) protecting group solid-phase peptide synthesis method, which produced a high-quality lipid at a moderately good yield. We then prepared Man-$(SG)_5$/PEGylated liposomes using a post-insertion technique to insert Man(S)-$(SG)_5$-SSK-K$(Pal)_2$ into the PEGylated liposomes. *In vitro* cell investigations revealed that the Man-$(SG)_5$/PEGylated liposomes effectively associated with mouse peritoneal macrophages by interacting with the mannose receptors. The results suggest that we produced a novel high-quality, highly functional mannosylated lipid that is suitable for clinical drug delivery applications.

1. Introduction

A number of anticancer drugs have been developed; however, cancer is still a major threat to human health worldwide. Recent studies have revealed that heterogeneity in the tumor microenvironment—for example in gene expression, cellular morphology, metabolic activity, metabolism, motility, or metastatic potential—limits the therapeutic effects of anticancer drugs, and may cause drug resistance (Marusyk and Polyak, 2010). To overcome these heterogeneities, the use of nanoparticle-based drug delivery system (DDS) carriers—such as liposomes, polymeric micelles, and nanogels—has attracted attention as a rational approach to cancer treatment (Friedman et al., 2013; Srinivasarao

et al., 2015). To date, active tumor-targeting liposomes have been created using functional lipids grafted with ligands that are directed toward specific cancer cell receptors, or using polymers that are responsive toward stimuli such as temperature, pH, and enzymes (Fumoto and Kawakami, 2014; Hagimori et al., 2017). However, the production of DDS carriers with high functionality for clinical applications presents a challenge owing to the poor quality of the functional lipids and difficulties arising from the preparation method with regard to reproducibility (Altınoglu et al., 2015; Gerasimov et al., 1999). Therefore, there is a great demand for high functionality and quality (HFQ) lipids for clinical DDS applications that can be prepared using a simple method.

Mannose receptors are C-type lectin receptors that are expressed on the surfaces of macrophages, and have carbohydrate recognition domains bound by mannose (Allavena et al., 2010; Irache et al., 2008). They have potential roles in both innate and adaptive immune responses, and are associated with inflammatory and infectious diseases (Allavena et al., 2010; Irache et al., 2008). Furthermore, mannose receptors are highly expressed in tumor-associated macrophages that are related to tumor invasion, proliferation, and metastasis in tumor microenvironments (Qian and Pollard, 2010). Several macrophage-targeted liposomes grafted with mannose as a ligand have been developed for cancer treatment (Kono, et al., 2014; Matsui, et al., 2010; Un et al., 2010a, b; Vinogradov et al., 2014). Poly(ethylene glycol) (PEG) is generally used as a polymeric steric stabilizer to reduce uptake by the reticuloendothelial system (RES) and prolong circulation in the blood (Allen et al., 1991; Shibata et al., 2013). Using PEG as a spacer, ligands including mannose have also been conjugated to the ends of PEG-lipids. However, in some PEGylated nanoparticles, the display of mannose on the surface of the liposome is hindered because it becomes embedded in the PEG layer; this inhibits sufficient uptake of the nanoparticles (Hagimori et al., 2017). Moreover, it is difficult to separate pure ligand-PEG-lipids because PEG has a broad molecular weight distribution (Shibata et al., 2013). To improve the functionality and quality of ligand-conjugated lipids, we have recently developed HFQ lipids using a serine–glycine (SG) repeat peptide instead of the PEG spacer (Suga et al., 2017). We selected a short peptide (KCCYSL; abbreviated to KCC) for human epidermal growth factor receptor-2

(HER2), and obtained KCC-$(SG)_{5,7}$-lipids with a single molecular weight. Because the HER2-targeted peptide ligand was efficiently displayed outside the PEG layer, the uptake of KCC-$(SG)_{5,7}$/PEGylated liposomes was dramatically enhanced in HER2-positive breast cancer cells.

In the present study, we developed a novel mannosylated HFQ lipid with an $(SG)_5$ spacer for clinically available macrophage-targeted liposomes. Microfluidic devices such as the NanoAssemblr platform can simplify preparation of liposomes for clinical applications (Dong, et al., 2017). Regarding application for these devices, high dispersibility of HFQ lipids in water should also be considered. However, there have been few reports on the dispersibility of HFQ lipids in water. Therefore, we attempted to design a water-dispersible mannosylated HFQ lipid by simulating the net charge of lipids, and synthesized Man(S)-$(SG)_5$-SSK-$K(Pal)_2$ from *N*-Fmoc-*O*-(2,3,4,6-tetra-*O*-acetyl-α,β-D-mannopyranosyl)-L-serine using only a fluorenylmethyloxycarbonyl (Fmoc) protecting group solid-phase peptide synthesis method. We applied Man(S)-$(SG)_5$-SSK-$K(Pal)_2$ to Man-$(SG)_5$/PEGylated liposomes, and investigated *in vitro* its cellular association and intracellular distribution in mouse peritoneal macrophages.

2. Materials and methods

2.1. Materials

We purchased D-mannose, CH_3ONa, and 1-methyl-2-pyrrolidone (NMP) from Wako Pure Chemical Industries (Osaka, Japan). We purchased Fmoc-protected amino acids, 2-(1*H*-benzotriazole-1-yl)-1,1,3,3-tetramethyluronium hexafluorophosphate (HBTU), *N*,*N*-diisopropylethylamine (DIPEA), triisopropylsilane (TIS), and Rink Amide AM resin from Merck (Darmstadt, Germany). We purchased 1-hydroxybenzotriazole (HOBT) from the Peptide Institute, Inc. (Osaka, Japan). Thioglycolate medium was purchased from Nissui Pharmaceutical Co. (Tokyo, Japan). We purchased 1,2-distearoyl-sn-glycero-3-phosphocholine (DSPC) and rhodamine-1,2-dioleoyl-sn-glycero-3-phosphoethanolamine (Rhod-DOPE) from Avanti Polar Lipids (Alabaster, AL, USA). We purchased

1,2-distearoyl-sn-glycero-3-phosphoethanolamine-*N*-[amino(polyethylene glycol)-2000] (NH_2-PEG_{2000}-DSPE) and 1,2-distearoyl-sn-glycero-3-phosphoethanolamine-*N*-[methoxy (polyethylene glycol)-2000] ($mPEG_{2000}$-DSPE) from NOF Co. (Tokyo, Japan). Palmitic acid (Pal) and cholesterol were purchased from Nacalai Tesque Inc. (Kyoto, Japan). All other chemicals were of the highest purity available. We used a peptide calculator produced by Bachem (Bubendorf, Switzerland) to determine the theoretical physicochemical properties of the peptides.

*2.2. Synthesis of cyanomethyl-2,3,4,6-tetra-*O*-acetyl-1-thiomannoside (CME-thiomannoside)*

CME-thiomannoside was prepared as described previously (Lee et al., 1976). Briefly, 70% perchloric acid was added drop-wise to a solution of D-mannose (25 g) in acetic anhydride (100 mL), and the reaction mixture was stirred overnight. We then added 25% HBr/CH_3COOH (50 mL), and stirred the mixture overnight under cool conditions. We obtained the acetohalo sugar after separation and evaporation. We then added thiourea to a solution of the acetohalo sugar in dry acetone, and refluxed the mixture for 15 min. Chloroacetonitrile, K_2CO_3, and $NaHSO_3$ were added to the solution, and the mixture was stirred for 2 h over ice. We obtained 8.98 g of cyanomethyl-2,3,4,6-tetra-*O*-acetyl-1-thiomannoside (CME-thiomannoside) after separation and evaporation. The CME-thiomannoside was confirmed by fast-atom bombardment mass spectrometry (FAB-MS) analysis. The mass-to-charge ratio (m/z) according to FAB-MS was 404 [M + H^+]. According to high-resolution mass spectrum (HRMS) FAB, the m/z ratios for $C_{16}H_{21}NO_9S$ [M + H^+] were 404.1015 (calculated) and 404.1016 (found).

2.3. Synthesis of Man-PEG_{2000}-DSPE

Man-PEG_{2000}-DSPE was prepared according to the method reported previously (Un et al., 2010b). We obtained 2-imino-2-methoxyethyl-1-thiomannoside (IME-thiomannoside) by stirring CME-thiomannoside with 0.01 M CH_3ONa/MeOH for

24 h at room temperature (RT) (Lee et al., 1976). IME-thiomannoside (10 eq) and NH_2-PEG_{2000}-DSPE (1 eq) were reacted in pyridine containing trimethylamine for 24 h. After concentrating by evaporation, water was added to the residue. The mixture was then dialyzed for 24 h (molecular weight (MW) cut-off of 6–8 kDa) and lyophilized. Man-PEG_{2000}-DSPE was confirmed by matrix-assisted laser desorption/ionization time-of-flight mass spectroscopy (MALDI-TOF-MS).

2.4. Synthesis of Man-$(SG)_5$-SSR-$K(Pal)_2$

K-$(SG)_5$-SSR-$K(Pal)_2$ was prepared using an Fmoc solid-phase peptide synthesis method. The Fmoc groups were deprotected with 20% piperidine for 20 min, and coupling reactions using Fmoc amino acids were performed with HBTU/HOBT/DIPEA for 30 min. The unreacted amino groups were capped with 25% acetic anhydride. Following the coupling reaction to form Fmoc-Lys(Fmoc)-OH, the Fmoc groups were deprotected and palmitic acid (10 eq) was reacted twice with HBTU/HOBT/DIPEA for 4 h. A solution comprising trifluoroacetic acid (TFA)/TIS/H_2O (94/2.5/2.5, v/v/v) was added and reacted for 3 h to cleave from the resin. Dialysis of the crude product for 5 days (MW cut-off of 6–8 kDa) followed by lyophilization yielded $(SG)_5$-SSR-$K(Pal)_2$. IME-thiomannoside (10 eq) and K-$(SG)_5$-SSR-$K(Pal)_2$ (1 eq) were reacted for 24 h in a mixture comprising pyridine (2 mL), dimethyl sulfoxide (1 mL), and trimethylamine (20 μL). The products were concentrated by evaporation and water was added to the residue. This was followed by dialysis for 48 h (MW cut-off of 6–8 kDa) and lyophilization. The reaction mixture was analyzed using a high-performance liquid chromatography (HPLC) system with a reversed-phase column (COSMOSIL 5C_{18}-AR-II 4.6 × 250 mm) at a flow rate of 0.5 mL/min. The mobile phase comprised a linear gradient of solvent A (0.1% TFA in acetonitrile) and solvent B (0.1% TFA in water) that increased from 50% solvent A to 100% solvent A over 40 min. The product was confirmed by MALDI-TOF-MS.

*2.5. Synthesis of N-Fmoc-O-(2,3,4,6-tetra-*O*-acetyl-α,β-D-mannopyranosyl)-L-serine (Kragol & Otvos, 2001)*

We synthesized α,β-mannose pentaacetate by reacting α,β-D-mannose (490 mg) with acetic anhydride in pyridine. We added $BF_3 \cdot Et_2O$ (24.6 mmol) to a solution of α,β-mannose pentaacetate (2.72 mmol) and Fmoc-serine-OH (3.28 mmol) in CH_3CN, and stirred the mixture for 4 h in the dark. After adding CH_2Cl_2 (160 mL), the organic layer was washed with 1 M HCl (20 mL) and H_2O (20 mL), dried over $MgSO_4$, and concentrated by evaporation. The product was then lyophilized. The reaction mixture was purified using a HPLC system with a reversed-phase column (COSMOSIL $5C_{18}$-AR-II 20 × 250 mm) at a flow rate of 5 mL/min. The mobile phase comprised a linear gradient of solvent A (0.1% TFA in 90% acetonitrile and 10% water) and solvent B (0.1% TFA in water) that increased from 50% solvent A to 100% solvent A over 30 min. MS (FAB) m/z: 658 [M + H^+]; HRMS (FAB) for $C_{32}H_{36}NO_{14}$ [M + H^+] 658.2125 (calculated), 658.2136 (found).

2.6. Synthesis of Man(S)-$(SG)_5$-SSK-K$(Pal)_2$

We prepared Man(S)-$(SG)_5$-SSK-K$(Pal)_2$ using an Fmoc solid-phase peptide synthesis method. The reaction to produce *N*-Fmoc-*O*-(2,3,4,6-tetra-*O*-acetyl-α,β-D-mannopyranosyl)-L-serine using HBTU/HOBT/DIPEA was carried out over 4 h, whereas the reactions involving the other amino acids were carried out over 30 min. The unreacted amino groups were capped with 25% acetic anhydride. Following the coupling of Fmoc-Lys(Fmoc)-OH, the Fmoc groups were deprotected, palmitic acid (10 eq) was reacted twice with HBTU/HOBT/DIPEA for 4 h, and deacetylation was preformed four times with 0.01 M CH_3ONa/NMP-MeOH (17:3) for 30 min. Cleavage from the resin and dialysis of the crude product were carried out according to the methods described above. The reaction mixture was analyzed using a HPLC system with a reversed-phase column (COSMOSIL 5C18-AR-II 4.6 × 250 mm) at a flow rate of 0.5 mL/min. The mobile phase comprised a linear gradient of solvent A (0.1% TFA in acetonitrile) and solvent B (0.1% TFA in water) that increased from 50% solvent A to 100% solvent A over 60 min.

2.7. Preparation of Man-$(SG)_5$/PEGylated liposomes

We dissolved DSPC, cholesterol, and $mPEG_{2000}$-DSPE in methanol, and evaporated the resulting solution to prepare dried lipid films. We then added 0.5 mol% rhodamine-DOPE to label the liposomes. The dried lipid films were hydrated with 2 mL of distilled water at 65°C for 10 min. The PEGylated liposomes were sonicated for 3 min in a probe type sonicator, and filtered through a 0.45-μm filter (Nihon-Millipore, Tokyo, Japan). We added 67.2 μL (6 mol% of the total lipid content) or 100.8 μL (9 mol% of the total lipid content) of 2 mg/mL Man(S)-$(SG)_5$-SSK-$K(Pal)_2$ in H_2O to 500 μL of the PEGylated liposomes (2 mg/mL), and incubated the mixture at 60°C for 1 h. We obtained Man-$(SG)_5$/PEGylated liposomes after diluting with phosphate-buffered saline (PBS). The particle sizes and ζ-potentials of the Man-$(SG)_5$/PEGylated liposomes in PBS were measured using a Zetasizer Nano ZS system (Malvern Instruments, Ltd., Malvern, United Kingdom).

2.8. Preparation of mannosylated PEGylated liposomes

We dissolved DSPC, cholesterol, $mPEG_{2000}$-DSPE, and Man-$mPEG_{2000}$-DSPE in methanol, and evaporated the resulting solution to prepare dried lipid films. We then added 0.5 mol% rhodamine-DOPE to label the liposomes. The dried lipid films were hydrated with 2 mL of PBS at 65°C for 10 min. The Man-$PEG_{2,000}$/PEGylated liposomes were sonicated for 3 min in a probe type sonicator, and filtered through a 0.45-μm filter (Nihon-Millipore, Tokyo, Japan). The particle sizes and ζ-potentials of the Man-$PEG_{2,000}$/PEGylated liposomes in PBS were measured using a Zetasizer Nano ZS system (Malvern Instruments, Ltd., Malvern, United Kingdom).

2.9. Animal experiments

All animal studies were conducted in accordance with the experimental guidelines provided by Nagasaki University, and the experiments were approved by the Institutional Animal Care and Use Committee of Nagasaki University.

2.10. Harvest and culture of mouse peritoneal macrophages

Four-week-old male ICR mice were supplied by CLEA Japan Inc. (Tokyo, Japan). We

used the methods reported by Un et al. (2010a) to culture and harvest the mouse peritoneal macrophages. A solution of 2.9% thioglycolate medium (1 mL) was intraperitoneally administrated to the mice. Four days later, the collected macrophages were washed and suspended in Roswell Park Memorial Institute 1640 (RPMI-1640) medium containing 10% fetal bovine serum, and the mouse peritoneal macrophages (0.5 mL; 1.0×10^6 cells/mL) were applied to a 24-well plate. After incubation for 2 h at 37°C in a 5% CO_2 atmosphere, the floating cells were removed, and the macrophages were incubated for another 3 days.

2.11. Cellular association study using flow cytometry

Fluorescently labelled liposomes were prepared by adding 0.5 mol% Rhod-DOPE. After the mouse peritoneal macrophages had been cultured in 24-well plates for 72 h (2.6×10^5 cells/cm^2), they were incubated with serum-free RPMI-1640 containing liposomes (25 μM) (PEGylated liposomes, Man-$PEG_{2,000}$/PEGylated liposomes, or Man-$(SG)_5$/PEGylated liposomes) for 3 h at 37°C in a 5% CO_2 atmosphere, and analyzed by flow cytometry (BD LSRFortessa, BD Biosciences, San Diego, CA, USA).

2.12. Intracellular distribution study using a confocal laser scanning microscope (CLSM)

The mouse peritoneal macrophages were cultured in 35-mm glass-based dishes (2.5×10^5 cells/cm^2) for 72 h, and incubated with serum-free RPMI-1640 containing liposomes (25 μM) (PEGylated liposomes, Man-$PEG_{2,000}$/PEGylated liposomes, or Man-$(SG)_5$/PEGylated liposomes) for 3 h at 37°C in a 5% CO_2 atmosphere. The nuclei and lysosomes were stained with 4′,6-diamidino-2-phenylindole (DAPI) (Sigma-Aldrich Co., Milwaukee, WI, USA) and LysoTracker Green (Invitrogen Co., Carlsbad, CA, USA), respectively, in preparation for analysis using a CLSM (LSM 710, Carl Zeiss, Oberkochen, Germany).

2.13. Investigation of the competitive inhibition of the mannose receptor by mannan using flow cytometry

After the mouse peritoneal macrophages had been cultured in 24-well plates (2.6×10^5 cells/cm^2) for 72 h, the cells were washed twice with PBS, and pre-incubated for 30 min with serum-free RPMI-1640 containing mannan (1 mg/mL). They were then incubated with serum-free RPMI-1640 containing liposomes (25 μM) (PEGylated liposomes, Man-PEG2,000/PEGylated liposomes, or Man-HFQ liposomes) in the presence of mannan (1 mg/mL) for 3 h at 37°C in a 5% CO_2 atmosphere. The cells were analyzed by flow cytometry (BD LSRFortessa, BD Biosciences, San Diego, CA, USA).

2.14. Investigation of the competitive inhibition of the mannose receptor by mannan using a CLSM

After the mouse peritoneal macrophages had been cultured in 35-mm glass-based dishes (2.5×10^5 cells/cm^2) for 72 h, the cells were washed twice with PBS, and incubated with serum-free RPMI-1640 containing mannan (1 mg/mL). They were then incubated with serum-free RPMI-1640 containing liposomes (25 μM) (PEGylated liposomes, Man-$PEG_{2,000}$/PEGylated liposomes, or Man-HFQ liposomes) in the presence of mannan (1 mg/mL) for 3 h at 37°C in a 5% CO_2 atmosphere. The nuclei and lysosomes were stained with DAPI (Sigma-Aldrich Co., Milwaukee, WI, USA) or LysoTracker Green (Invitrogen Co., Carlsbad, CA, USA), respectively, in preparation for analysis using a CLSM (LSM 710, Carl Zeiss, Oberkochen, Germany).

2.15. Statistical analysis

The data are expressed as the means ± SD. The statistical significance of differences between groups was tested by analysis of variance. The Tukey–Kramer test was used to compare differences between multiple groups.

3. Results

3.1. Synthesis of water-dispersible mannosylated lipids

Peptide sequences including polar amino acids (glutamic acid or arginine) or elongated SG spacers were used to confer a high degree of water dispersibility on the mannosylated lipids, and net peptide charges were simulated using a Bachem peptide

calculator (Fig. 1). The net charges of K-$(SG)_5$-SS-E-K$(pal)_2$ and K-$(SG)_{10}$-SS-E-K$(pal)_2$ were zero. The introduction of one or two glutamic acid (E) residues between the C-terminal lysine and $(SG)_5$ conferred a net negative charge. A positive charge was conferred on K-$(SG)_5$-SS-E-K$(pal)_2$ by replacing the glutamic acid (E) residue with arginine (R) to form K-$(SG)_5$-SS-R-K$(pal)_2$. These lipids were produced using an Fmoc solid-phase peptide synthesis method, and their dispersibility in water was evaluated. Only the positively charged lipid K-$(SG)_5$-SS-R-K$(pal)_2$ had high dispersibility in water at a concentration of more than 0.2 mM. As shown in Fig. 2, the liquid-phase conjugation of K-$(SG)_5$-SS-R-K$(pal)_2$ with IME-thiomannoside was carried out in pyridine containing dimethyl sulfoxide and trimethylamine for 24 h, and a mannosylated lipid, Man-$(SG)_5$-SSR-K$(Pal)_2$, was obtained at a yield of 8.2%. Analysis of the product using a HPLC-UV system and mass spectrometry revealed an abundance of peaks attributable to by-products (Fig. S1, S2).

We included mannose conjugation in the Fmoc solid-phase peptide synthesis method to improve the yield and quality of the mannosylated lipids. We designed a novel mannosylated lipid, Man(S)-$(SG)_5$-SSK-K$(Pal)_2$, with a positive net charge (Fig. 3). An Fmoc-mannose-serine (Man(S)) derivative, *N*-Fmoc-*O*-(2,3,4,6-tetra-*O*-acetyl-α,β-D-mannopyranosyl)-L-serine, was synthesized via a two-step reaction from mannose, and the yield was 17%. As shown in Fig. 4, we reacted the carboxyl group of the Fmoc-mannose-serine residue with the amine group of the resin using HBTU/HOBT/DIPEA. After removing the Fmoc group using piperidine, the peptide chain, which included $(SG)_5$-SSK-K, was elongated and ultimately coupled with palmitic acid. After cleavage from the resin, deprotection of the Fmoc groups of the amino acids and the acetyl groups of mannose produced the desired Man(S)-$(SG)_5$-SSK-K$(pal)_2$ at a yield of 40.8%. According to HPLC-UV and mass spectrometry analysis, the obtained product had high purity (Fig. S3, S4).

3.2. Preparation of Man-$(SG)_5$/PEGylated liposomes

We used sonication and post-insertion methods to prepare mannosylated HFQ liposomes. We added Man(S)-$(SG)_5$-SSK-K$(pal)_2$ in water to the PEGylated liposomes

and incubated the mixture at 60°C for 1 h to produce Man-$(SG)_5$/PEGylated liposomes with three different degrees of mannosylation (3, 6, and 9%). We also prepared mannosylated PEGylated liposomes (Man-$PEG_{2,000}$/PEGylated liposomes) with three different degrees of mannosylation (3, 6, and 9%), according to a previously reported method. The particle sizes and ζ-potentials of the liposomes are summarized in Table 1. Except for the ungrafted PEGylated liposomes and the 3% Man-$(SG)_5$/PEGylated liposomes, the size of the liposomes ranged from 93.8 to 123.5 nm. The ζ-potentials of Man-$(SG)_5$/PEGylated liposomes were maintained at a slightly negative charge, whereas those of the Man-$PEG_{2,000}$/PEGylated liposomes had an increasingly positive charge according to the degree of mannosylation.

3.3. Cellular association study

To compare cellular association in the ungrafted PEGylated liposomes, the Man-$PEG_{2,000}$/PEGylated liposomes, and the Man-$(SG)_5$/PEGylated liposomes, the liposomes were labeled with rhodamine, and the fluorescence of the labeled liposomes in the cells was investigated by flow cytometry. The flow cytometry profiles and mean fluorescence intensities are shown in Fig. 5. The Man-$(SG)_5$/PEGylated liposomes exhibited greater fluorescence intensity than the ungrafted PEGylated and Man-$PEG_{2,000}$/PEGylated liposomes in the mouse peritoneal macrophages. In particular, there was significant enhancement of the cellular association in the 9% grafted Man-$(SG)_5$/PEGylated liposomes. In contrast, cellular association in the Man-$PEG_{2,000}$/PEGylated liposomes with 6 or 9% mannosylation was reduced compared with the ungrafted PEGylated liposomes.

3.4. Intracellular distribution study

As shown in Fig. 6, we investigated the intracellular distribution of ungrafted PEGylated liposomes, Man-$PEG_{2,000}$/PEGylated liposomes, and Man-$(SG)_5$/PEGylated liposomes in mouse peritoneal macrophages using a CLSM. Following incubation of the Man-$(SG)_5$/PEGylated liposomes for 1 h, we observed bright red rhodamine fluorescence from the labelled Man-$(SG)_5$/PEGylated liposomes, especially in the 9%

grafted Man-$(SG)_5$/PEGylated liposomes. Furthermore, the red fluorescence was colocalized with green fluorescence from LysoTracker Green (a lysosomal marker). In contrast, we observed weak rhodamine fluorescence in the ungrafted PEGylated and Man-$PEG_{2,000}$/PEGylated liposomes.

3.5. Cellular association and distribution with mannan

We confirmed the target efficacy of the Man-$(SG)_5$/PEGylated liposomes using mannan as a mannose receptor ligand (Fig. 7). After the mouse peritoneal macrophages had been incubated with serum-free RPMI-1640 containing 1 mg/mL mannan for 30 min, the medium was replaced with fresh medium containing Man-$(SG)_5$/PEGylated liposomes (25 μM) grafted with 6 or 9% mannose and 1 mg/mL mannan. The mixture was then incubated for 3 h. Flow cytometry quantification studies revealed that cellular association in the 6 and 9% mannose-grafted Man-$(SG)_5$/PEGylated liposomes was significantly reduced by the addition of 1 mg/mL mannan (Fig. 7A). We also carried out CLMS studies with 1 mg/mL mannan using 9% mannose-grafted Man-$(SG)_5$/PEGylated liposomes in mouse peritoneal macrophages (Fig. 7B), and found that the localization of the Man-$(SG)_5$/PEGylated liposomes in lysosomes was inhibited by mannan.

4. Discussion

The objective of the present study was to develop a novel and clinically applicable liposome that can target the mannose receptor. Therefore, we designed and synthesized water-dispersible HFQ lipids, prepared Man-$(SG)_5$/PEGylated liposomes as mannose receptor-targeted HFQ liposomes, and evaluated their *in vitro* efficacy in mouse peritoneal macrophages. Several studies have demonstrated that mannosylated liposomes are promising carriers for anticancer drugs, proteins, NF-κB, and plasmid DNA (Fukasawa, et al., 1998; Kawakami and Hashida, 2014; Kono, et al., 2014; Matsui et al., 2010; Un, et al., 2010a, b; Vinogradov et al., 2014). A number of mannosylated liposomes with PEG surface coatings have been designed because long, flexible PEG chains stabilize nanoparticles (Allen et al., 1991). It has been reported that the PEG layer serves as a barrier (Hagimori et al., 2017; Suga et al., 2017), prevents the display

of mannose, and reduces the interaction between the liposome and the target cell. To overcome these drawbacks, Zhu et al. used an acid-sensitive bond to efficiently target tumor-associated macrophages (Zhu et al., 2013). In this system, the nanoparticles shed their PEG coatings in acidic tumor microenvironments; subsequently the mannosylated nanoparticles associate via mannose–mannose receptor recognition. In the present study, we used serine–glycine (SG) repeat peptides to efficiently display the mannose ligand outside the PEG layer. The dispersibility of the lipid in water is a crucial factor in the post-insertion technique that enables the insertion of lipids into commercially available liposomes that are suitable for clinical DDSs using microfluidic devices. Therefore, we attempted to design and synthesize a HFQ lipid with high dispersibility in water.

Previously our group reported mannose receptor-targeted liposomes comprising Man-PEG_{2000}-DSPE, which were synthesized using the liquid phase synthesis method, namely the reaction of NH_2-PEG_{2000}-DSPE with IME-thiomannoside in pyridine (Un, et al., 2010b). To apply this liquid phase synthesis method, we designed $(SG)_n$ peptide sequences that included glutamic acid as an acidic amino acid, arginine as a basic amino acid, and a repeat sequence of SG for hydrophilicity; we simulated net charge using a Bachem peptide calculator, and synthesized five lipids constructed from $(SG)_n$ peptide sequences and palmitic acid (Fig. 1). Only the positively charged lipid, K-$(SG)_5$-SSR-K$(pal)_2$, exhibited high dispersibility in water. Because deionized water is slightly acidic, the γ-carboxyl groups of the glutamic acid residues were protonated, resulting in glutamic acid residues that did not enhance the dispersibility of the lipids in water. Furthermore, the SG repeat sequence did not improve the dispersibility of the lipids in water. The mannosylated lipid, Man-$(SG)_5$-SSR-K$(pal)_2$, was synthesized through the liquid phase reaction of K-$(SG)_5$-SSR-K$(pal)_2$ and IME-thiomannoside in pyridine (Fig. 2). However, there were many byproducts, and the yield of Man-$(SG)_5$-SSR-K$(pal)_2$ was only 8.2%. Although the imidoester of IME-thiomannoside is an amine-reactive crosslinking group, side-reactions are likely below pH 10 (Hand and Jencks, 1962). To suppress side-reactions and improve purity, we designed a novel lipid, Man(S)-$(SG)_5$-SSK-K$(pal)_2$, which comprised a mannose–serine residue and $(SG)_5$-SSK-K$(pal)_2$ (Fig. 3). A straightforward Fmoc

solid-phase peptide synthesis method using *N*-Fmoc-*O*-(2,3,4,6-tetra-*O*-acetyl-α,β-D-mannopyranosyl)-L-serine as a starting material produced a moderately good yield (40.8%) of high purity Man(S)-$(SG)_5$-SSK-$K(pal)_2$ (Fig. 4).

Macrophage-targeted Man-$(SG)_5$/PEGylated liposomes with different degrees of mannosylation (3, 6, and 9%) were prepared by sonication to reduce the size distribution of liposomes and post-inserting Man(S)-$(SG)_5$-SSK-$K(pal)_2$ into PEGylated liposomes. Physicochemical investigations of the ungrafted PEGylated liposomes, the Man-$PEG_{2,000}$/PEGylated liposomes, and the Man-$(SG)_5$/PEGylated liposomes revealed that their ultimate diameters were approximately 100 nm (Table 1). With regard to ζ-potentials, although the 6 and 9% mannosylated Man-$PEG_{2,000}$/PEGylated liposomes had positive charges, the Man-$(SG)_5$/PEGylated liposomes had weak negative charges. It has been reported that a weak negative charge on the nanoparticles can reduce non-specific binding (Chen, et al., 2010). Therefore, these results suggest that Man-$(SG)_5$/PEGylated liposomes possess favorable characteristics for *in vivo* applications. The flow cytometry studies revealed that cellular association was greater in the 6 or 9% mannosylated Man-$(SG)_5$/PEGylated liposomes than in the PEGylated liposomes and 6 or 9% mannosylated Man-$PEG_{2,000}$/PEGylated liposomes in mouse peritoneal macrophages (Fig. 5). This suggests that mannose ligands can be displayed outside the PEG layer of Man-$(SG)_5$/PEGylated liposomes using an $(SG)_5$ spacer. This finding agrees well with the results of our previous investigations into KCC-$(SG)_5$/PEGylated liposomes (Suga et al., 2017). The cationic Man-$PEG_{2,000}$/PEGylated liposomes exhibited lower cellular association than the anionic ungrafted PEGylated liposomes (Fig. 5). These quantitative results corroborate the reports that the uptake of cationic liposomes is lower than that of anionic liposomes in mouse peritoneal macrophages (Aramaki et al., 1995; Dadashzadeh et al., 2010). However, because it has been reported that positive charge on the surface of DDS carriers enhances cellular uptake (Fröhlich, 2012), charge and sequence optimization of Man-mPEG$_{2,000}$-DSPE might improve the cellular association of Man-$PEG_{2,000}$/PEGylated liposomes. To confirm intracellular distribution, we obtained

CLSM images of ungrafted PEGylated liposomes, Man-$PEG_{2,000}$/PEGylated liposomes, and Man-$(SG)_5$/PEGylated liposomes in mouse peritoneal macrophages (Fig. 6). In accordance with the results shown in Fig. 5, the CLSM images revealed that the Man-$(SG)_5$/PEGylated liposomes were internalized in macrophages more than the ungrafted PEGylated liposomes. Furthermore, co-staining with LysoTracker Green provided evidence that Man-$(SG)_5$/PEGylated liposomes can be localized in lysosomes via mannose receptor-mediated endocytosis. The lysosomal degradation of liposomes is one of the problems in drug delivery (Hagimori et al., 2017). Therefore, further studies will be required to improve the intracellular distribution of Man-$(SG)_5$/PEGylated liposomes in combination with methods facilitating intracellular lysosomal escape. The inhibitory study in the presence of excess mannan as a mannose receptor ligand indicated that the high uptake of Man-$(SG)_5$/PEGylated liposomes by mouse peritoneal macrophages is mediated by mannose receptors (Fig. 7).

5. Conclusions

We have developed a novel mannosylated HFQ lipid with an $(SG)_5$ spacer, Man(S)-$(SG)_5$-SSK-K$(pal)_2$, for macrophage-targeted liposomes. The lipid was synthesized using only a Fmoc solid-phase synthesis method with *N*-Fmoc-*O*-(2,3,4,6-tetra-*O*-acetyl-α,β-D-mannopyranosyl)-L-serine as a starting material, and the product had high purity and high dispersibility in water. Man-$(SG)_5$/PEGylated liposomes can be prepared by post-inserting the Man(S)-$(SG)_5$-SSK-K$(pal)_2$ into PEGylated liposomes. Moreover, Man-$(SG)_5$/PEGylated liposomes can be taken up by mannose receptor-mediated endocytosis in mouse peritoneal macrophages. Although further studies are needed to clarify the anticancer effect of drug loaded Man-$(SG)_5$/PEGylated liposomes, the data indicate that Man(S)-$(SG)_5$-SSK-K$(pal)_2$ has potential as a HFQ lipid for mannose receptor–targeted drug delivery systems.

Acknowledgements

This work was partly supported by JSPS KAKENHI Grant Number 18H03535 (S.K)

and Takeda Science Foundation (S.K).

References

Allavena, P., Chieppa, M., Bianchi, G., Solinas, G., Fabbri, M., Laskarin, G., Mantovani, A., 2010. Engagement of the mannose receptor by tumoral mucins activates an immune suppressive phenotype in human tumor-associated macrophages. Clin. Dev. Immunol. 2010, 547179. doi: 10.1155/2010/547179.

Allen, T. M., Hansen, C., Martin, F., Redemann, C., Yau-Young, A., 1991. Liposomes containing synthetic lipid derivatives of poly(ethylene glycol) show prolonged circulation half-lives in vivo. Biochim. Biophys. Acta, 1066, 29–36.

Altınoglu, S., Wang, M., Xu, Q., 2015. Combinatorial library strategies for synthesis of cationic lipid-like nanoparticles and their potential medical applications. Nanomedicine (London) 10, 643–657.

Aramaki, Y., Akiyama, K., Hara, T., Tsuchiya, S., 1995. Recognition of charged liposomes by rat peritoneal and splenic macrophages: effects of fibronectin on the uptake of charged liposomes, Eur. J. Pharmacol. 3, 63–70.

Chen, H., Yeh, J., Wang, L., Wu, X., Cao, Z., Wang, Y. A., Zhang, M., Yang, L., Mao, H., 2010. Reducing non-specific binding and uptake of nanoparticles and improving cell targeting with an antifouling PEO-*b*-PγMPS copolymer coating. Biomaterials 31, 5397–5407.

Dadashzadeh, S., Mirahmadi, N., Babaei, M.H., Vali, A.M., 2010. Peritoneal retention of liposomes: effects of lipid composition, PEG coating and liposome charge. J. Control, Release 148, 177–186.

Dong, Y.D., Tchung, E., Nowell, C., Kaga, S., Leong, N., Mehta, D., Kaminskas, L.M.,

Boyd, B. J., 2017. Microfluidic preparation of drug-loaded PEGylated liposomes, and the impact of liposome size on tumour retention and penetration. J. Liposome Res. 1–9.

Friedman, A.D., Claypool, S.E., Liu, R., 2013. The smart targeting of nanoparticles. Curr. Pharm. Des. 19, 6315–6329.

Fröhlich, E., 2012. The role of surface charge in cellular uptake and cytotoxicity of medical nanoparticles. Int. J. Nanomed. 7, 5577–5591.

Fukasawa, M., Shimizu, Y., Shikata, K., Nakata, M., Sakakibara, R., Yamamoto, N., Hatanaka, M., Mizuochi, T., 1998. Liposome oligomannose-coated with neoglycolipid, a new candidate for a safe adjuvant for induction of CD^{8+} cytotoxic T lymphocytes. *FEBS Lett.* 441, 353–356.

Fumoto, S., Kawakami, S., 2014. Combination of nanoparticles with physical stimuli toward cancer therapy. Biol. Pharm. Bull. 37, 212–216.

Gerasimov, O.V., Boomer, J.A., Qualls, M.M., Thompson, D.H., 1999. Cytosolic drug delivery using pH- and light-sensitive liposomes. Adv. Drug Deliv. Rev. 38, 317–338.

Hagimori, M., Fuchigami, Y., Kawakami, S., 2017. Peptide-based cancer-targeted DDS and molecular imaging. Chem. Pharm. Bull. 65, 618–624.

Hand, E.S., Jencks, W.P., 1962. Mechanism of the reaction of imido esters with amines. J. Am. Chem. Soc. 84, 3505–3514.

Irache, J.M., Salman, H.H., Gamazo, C., Espuelas, S., 2008. Mannose-targeted systems for the delivery of therapeutics. Expert Opin. Drug Deliv. 5, 703–724.

Kawakami, S., Hashida, M., 2014. Glycosylation-mediated targeting of carriers. J.

Control. Release 190, 542–555.

Kono. Y., Kawakami, S., Higuchi, Y., Maruyama, K., Yamashita, F., Hashida, M., 2014. Tumour-associated macrophages targeted transfection with NF-κB decoy/mannose-modified bubble lipoplexes inhibits tumour growth in tumour-bearing mice. J. Drug Target. 22, 439–449.

Kragol, G., Otvos, L., 2001. Orthogonal solid-phase synthesis of tetramannosylated peptide constructs carrying three independent branched epitopes. Tetrahedron 57, 957–966.

Lee, Y.C., Stowell, C.P., Krantz, M.J., 1976. 2-Imino-2-methoxyethyl 1-thioglycosides: new reagents for attaching sugars to proteins. Biochemistry 15, 3956–3963.

Marusyk, A., Polyak, K., 2010. Tumor heterogeneity: causes and consequences. Biochim. Biophys. Acta 1805, 105–117.

Matsui, M., Shimizu, Y., Kodera, Y., Kondo, E., Ikehara, Y., Nakanishi, H., 2010. Targeted delivery of oligomannose-coated liposome to the omental micrometastasis by peritoneal macrophages from patients with gastric cancer. Cancer Sci. 101, 1670–1677.

Qian, B.Z., Pollard, J.W., 2010. Macrophage diversity enhances tumor progression and metastasis. Cell 141, 39–51.

Shibata, H., Yomota, C., Okuda, H., 2013. Simultaneous determination of polyethylene glycol-conjugated liposome components by using reversed-phase high-performance liquid chromatography with UV and evaporative light scattering detection. AAPS PharmSciTech 14, 811–817.

Srinivasarao, M., Galliford, C.V., Low, P.S., 2015. Principles in the design of

ligand-targeted cancer therapeutics and imaging agents. Nat. Rev. Drug Discov. 14, 203–219.

Suga, T., Fuchigami, Y., Hagimori, M., Kawakami, S., 2017. Ligand peptide-grafted PEGylated liposomes using HER2 targeted peptide-lipid derivatives for targeted delivery in breast cancer cells: the effect of serine-glycine repeated peptides as a spacer. Int. J. Pharm. 521, 361–364.

Un, K., Kawakami, S., Suzuki, R., Maruyama, K., Yamashita, F., Hashida, M., 2010a. Enhanced transfection efficiency into macrophages and dendritic cells by a combination method using mannosylated lipoplexes and bubble liposomes with ultrasound exposure. Human Gene Therapy 21, 65–74.

Un, K., Kawakami, S., Suzuki, R., Maruyama, K., Yamashita, F., Hashida, M., 2010b. Development of an ultrasound-responsive and mannose-modified gene carrier for DNA vaccine therapy. Biomaterials 31, 7813–7826.

Vinogradov, S., Warren, G., Wei, X., 2014. Macrophages associated with tumors as potential targets and therapeutic intermediates. Nanomedicine (London) 9, 695–707.

Zhu, S., Niu, M., O'Mary, H., Cui, Z., 2013. Targeting of tumor-associated macrophages made possible by PEG-sheddable, mannose-modified nanoparticles. Mol. Pharmacol. 10, 3525–3530.

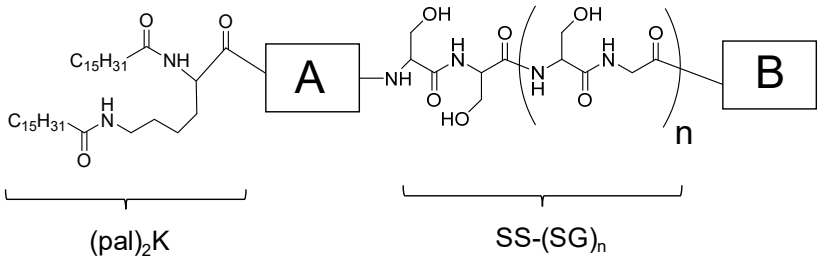

Lipid-peptide sequence	A	B	n	Net charge[a]
K-$(SG)_5$-SS-E-K$(pal)_2$	E	K	5	0
K-$(SG)_{10}$-SS-E-K$(pal)_2$	E	K	10	0
KE-$(SG)_5$-SS-E-K$(pal)_2$	E	EK	5	-2
KEE-$(SG)_5$-SS-E-K$(pal)_2$	E	EEK	5	-3
K-$(SG)_5$-SS-R-K$(pal)_2$	R	K	5	+2

[a]Net charge at pH 7.0 was calculated by Bachem peptide calculator

Fig. 1. The peptide sequence with polar amino acids (glutamic acid and arginine) or elongated SG spacer, and their net charge

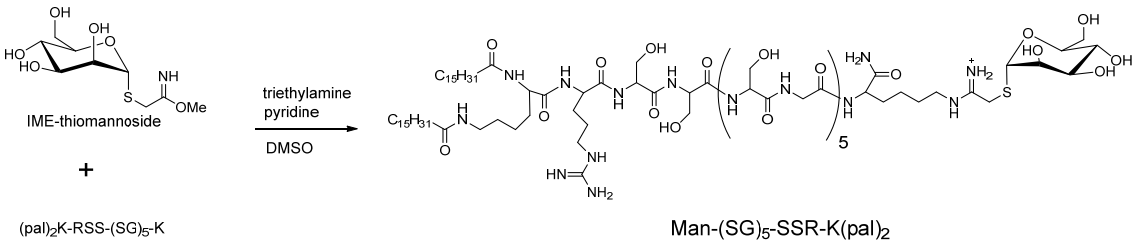

Fig. 2. Liquid-phase synthesis of Man-$(SG)_5$-SSR-K$(pal)_2$

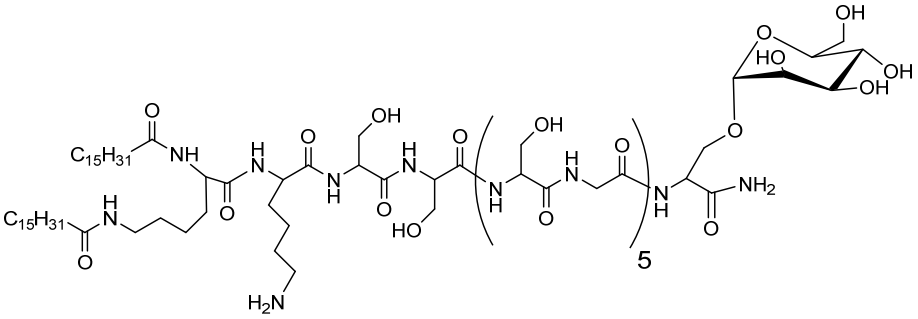

Fig. 3. Chemical structure of Man(S)-$(SG)_5$-SSK-$K(pal)_2$

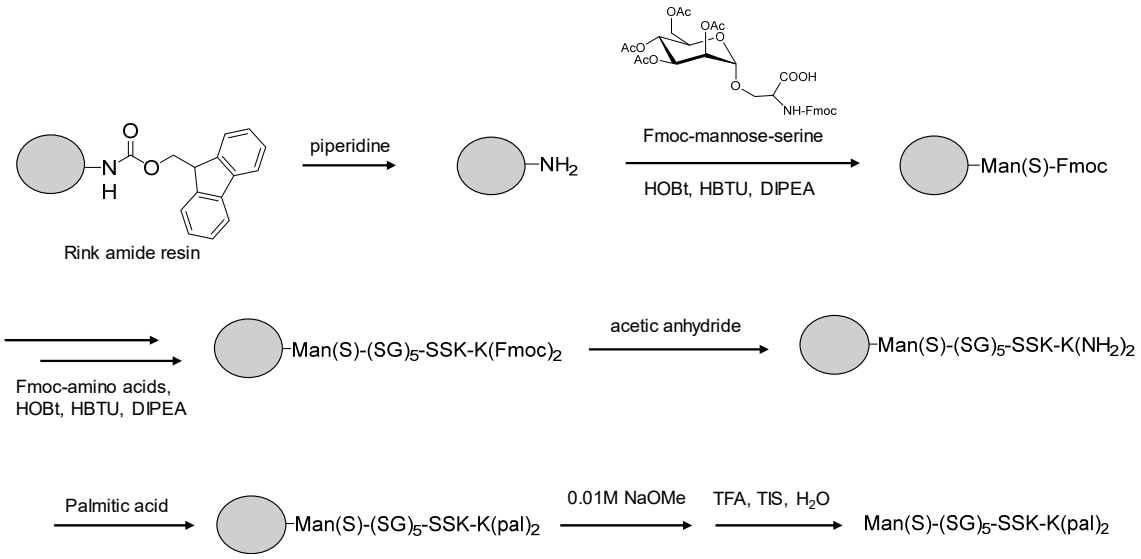

Fig. 4. Solid-phase synthesis of Man-$(SG)_5$-SSR-$K(pal)_2$

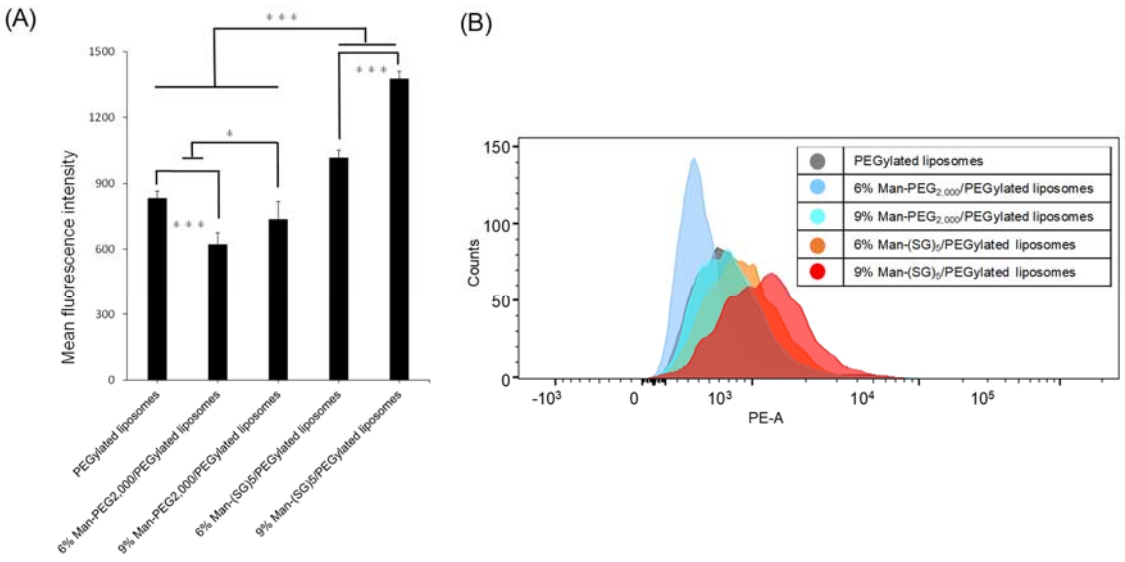

Fig. 5. Cellular association of PEGylated lyposomes, Man-PEG$_{2000}$/PEGylated liposomes, and Man-(SG)$_5$/PEGylated-liposome in peritoneal macrophage at a concentration 25 μM. Cell were incubated with liposomes for 3 h, then analyzed by flow cytometry. (A) Mean fluorescence intensity, (B) Histogram profiles. Date are represented as mean value ± SD (n = 5). ANOVA and Tukey's test. (*$P < 0.05$, ***$P<0.001$)

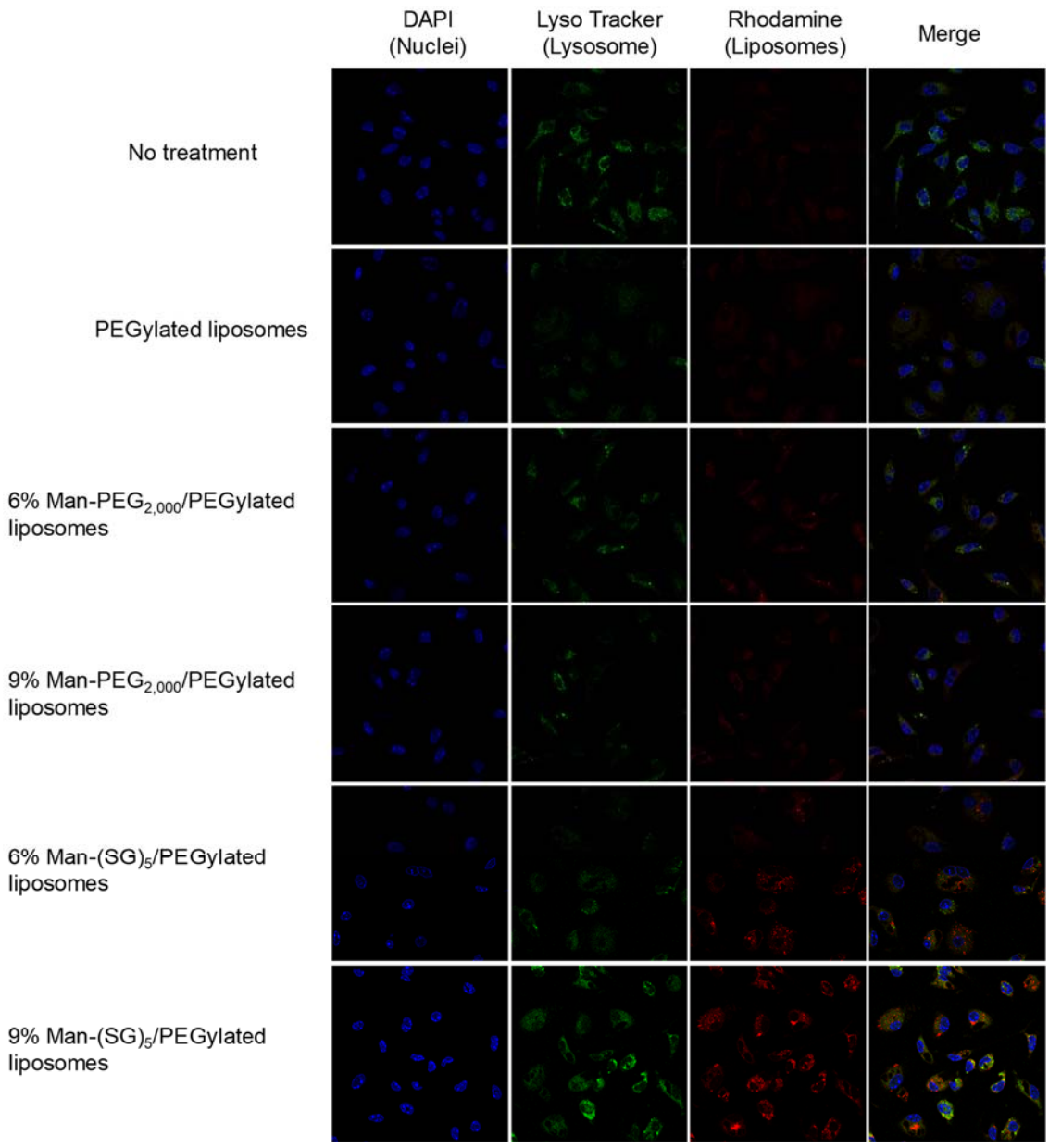

Fig. 6. Intracellular distribution studies of unmodified PEGylated liposomes, Man-PEG$_{2000}$/PEGylated liposomes, and Man-(SG)$_5$/PEGylated liposomes in mouse peritoneal macrophages. Nuclei (DAPI fluorescent signal: blue), Lysosome (LysoTracker signal: green), liposomes (Rhodamine fluorescent signal: red), and Merge: yellow signals indicate colocalization of liposomes and LysoTracker.

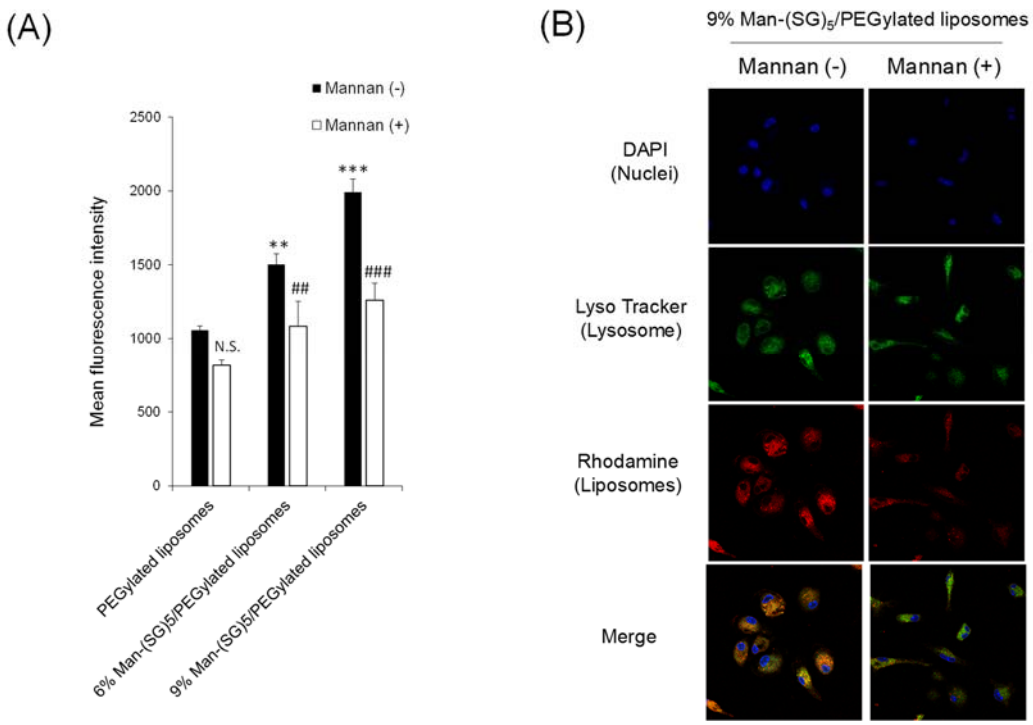

Fig. 7. Intracellular distribution of Man-$(SG)_5$/PEGylated liposomes with mannan (-) and mannan (+) in mouse peritoneal macrophages. (A) Quantification studies: Cells were incubated with PEGylated liposomes, 6% Man-$(SG)_5$/PEGylated liposomes, or 9% Man-$(SG)_5$/PEGylated liposomes without mannan as control (filled column) or with 1 mg/mL mannan (opened column). Each value represents the mean ± S.D. of three experiments. Statistically significant differences (**P<0.01, ***P<0.001) from a control of unmodified-liposomes, (##P<0.01; ###P<0.001) from a control (liposomes alone) for each group. N.S., not significant. (B) CLMS images: Cells were incubated with 9% Man-$(SG)_5$/PEGylated liposomes with mannan (-) and mannan (+). Nuclei (DAPI fluorescent signal: blue), Lysosome (LysoTracker signal: green), liposomes (Rhodamine fluorescent signal: red), and Merge: yellow signals indicate colocalization of liposomes and LysoTracker.

Table 1.The lipid composition, mean particle size and ζ potential of liposomes

Lipid composition (molar ratio)	Particle size (nm)	ζ-potential (mV)
PEGylate -liposomes (DSPC/Cholesterol/mPEG$_{2000}$-DSPE = 55/35/10)	157.4 ± 2.3	-4.15 ± 0.32
3% Man-PEG$_{2,000}$/PEGylated liposomes (DSPC/Cholesterol/mPEG$_{2000}$-DSPE/Man-PEG-DSPE = 55/35/7/3)	123.5 ± 1.3	-0.084 ± 0.97
6% Man-PEG$_{2,000}$/PEGylated liposomes (DSPC/Cholesterol/mPEG$_{2000}$-DSPE/Man-PEG-DSPE = 55/35/4/6)	105.3 ± 1.4	2.03 ± 0.73
9% Man-PEG$_{2,000}$/PEGylated liposomes (DSPC/Cholesterol/mPEG$_{2000}$-DSPE/Man-PEG-DSPE = 55/35/1/9)	93.8 ± 1.4	4.62 ± 0.81
3% Man-(SG)$_5$/PEGylated liposomes (DSPC/Cholesterol/mPEG$_{2000}$-DSPE/Man(S)-(SG)$_5$-SSK-K(Pal)$_2$ = 55/35/7/3)	213.9 ± 18.5	-1.82 ± 0.64
6% Man-(SG)$_5$/PEGylated liposomes (DSPC/Cholesterol/mPEG$_{2000}$-DSPE/Man(S)-(SG)$_5$-SSK-K(Pal)$_2$ = 55/35/7/6)	122.8 ± 3.6	-3.29 ± 0.71
9% Man-(SG)$_5$/PEGylated liposomes (DSPC/Cholesterol/mPEG$_{2000}$-DSPE/Man(S)-(SG)$_5$-SSK-K(Pal)$_2$ = 55/35/7/9)	121.7 ± 0.7	-3.57 ± 0.73

Results are expressed as the mean ± S.D. of three experiments.